Kanaani et al., http://www.jcb.org/cgi/content/full/jcb.200912101/DC1

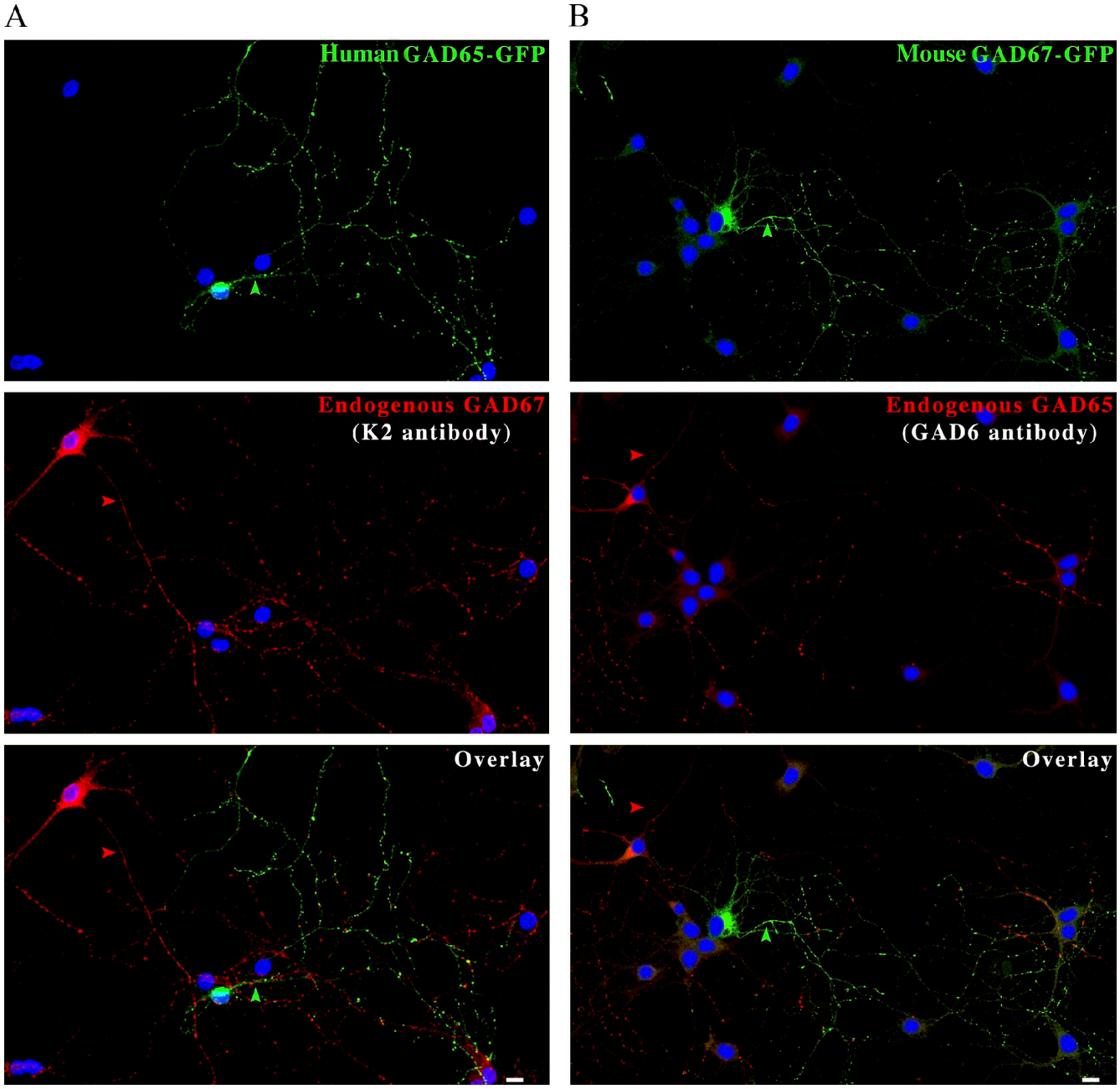

Figure S1. **The K2 rabbit polyclonal antibody is specific for GAD67, whereas the GAD6 monoclonal antibody is specific for GAD65 in immunofluorescence analyses of rat hippocampal neurons.** Confocal immunofluorescence analysis of hippocampal neurons transfected with either human GAD65-GFP (A) or mouse GAD67-GFP (B), and immunolabeled with antibodies for GFP (green) and either K2 polyclonal antibody to visualize endogenous GAD67 (A, red) or GAD6 monoclonal antibody to visualize endogenous GAD65 (B, red) and the nuclear stain DAPI (blue). The K2 antibody recognizes endogenous GAD67 in a GABAergic neuron (A, red) and does not cross-react with transfected GAD65-GFP in a neighboring non-GABAergic neuron (A, green). The GAD6 antibody recognizes only endogenous GAD65 in a GABAergic neuron (B, red) and does not cross-react with transfected mouse GAD67-GFP in a neighboring non-GABAergic neuron (B, green). Axons are indicated with arrowheads. Bars, 10 µm.

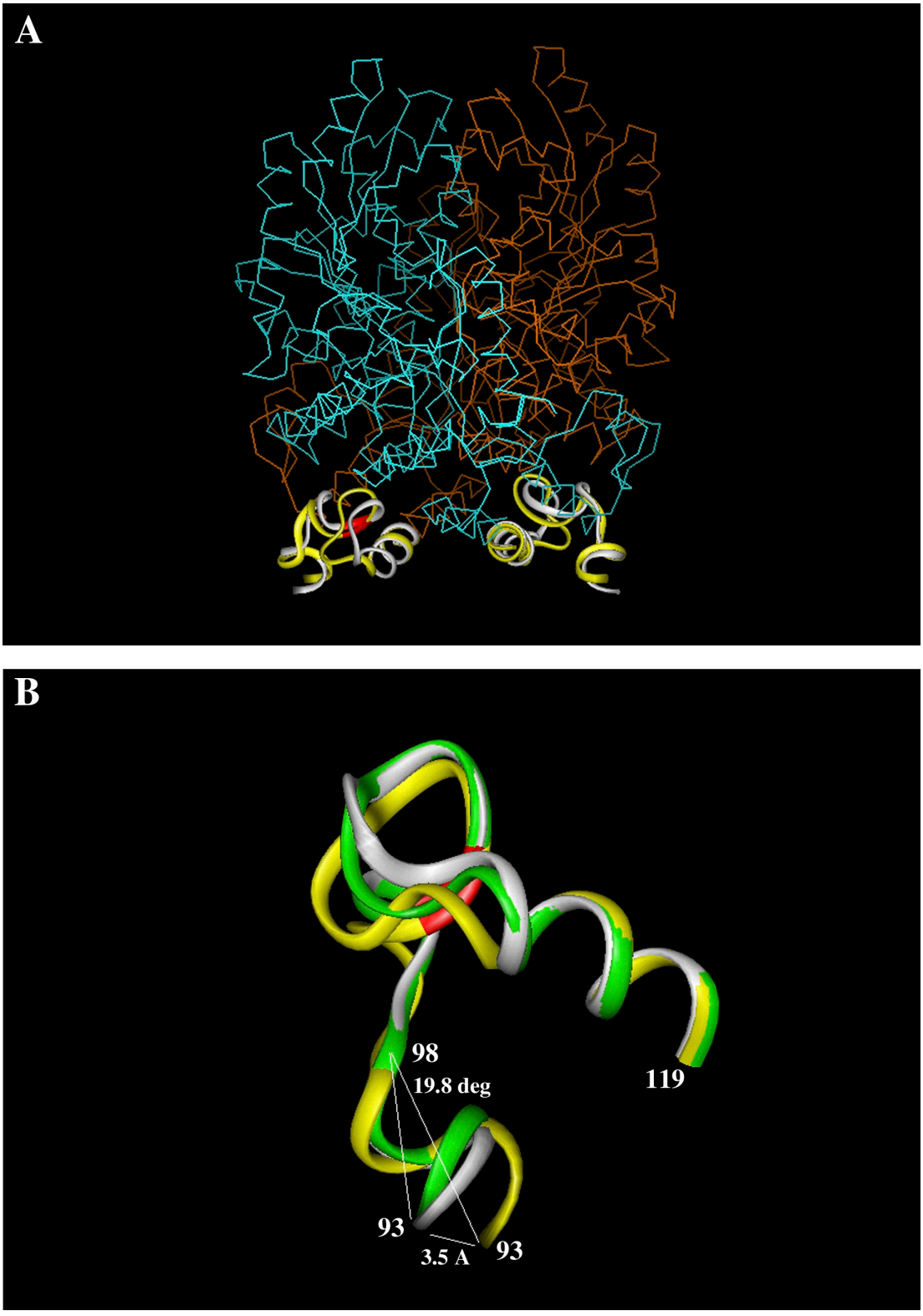

Figure S2. **Modeled changes in the structure of the human GAD67 dimer caused by an L103P mutation.** A rendering of the crystal model of GAD67 (PDB accession no. 2OKJ) illustrating the modeled change in the residue segment 93–119 resulting from the mutation L103P. (A) Except for their residue segments 93–119, which are shown as solid-oval ribbons, the two monomers comprising GAD67 are visualized as lines connecting carbon atoms. The A monomer is colored orange and the B monomer is colored cyan. The two nonmutated crystal segments 93–119 are colored white and the corresponding mutated ones are colored yellow. The location of residue 103 is colored red in the A monomer ribbons. (B) A close-up of the mutated and nonmutated segments 93–119, which also includes a segment that is colored green. It is the control segment that allows for the effects of isolation in modeling the mutation. Conformational changes due to modeled isolation and mutation are measured relative to this control segment. Shown is the distance between the corresponding carbon atoms of residue 93, and the angle subtended by these two atoms and the carbon atom of residue 98 of the control segment. The carbon atom of residue 98 in both the control and mutated segment shares a nearly common location. These two measurements illustrate the significant change in orientation of the control segment caused by the modeled mutation.

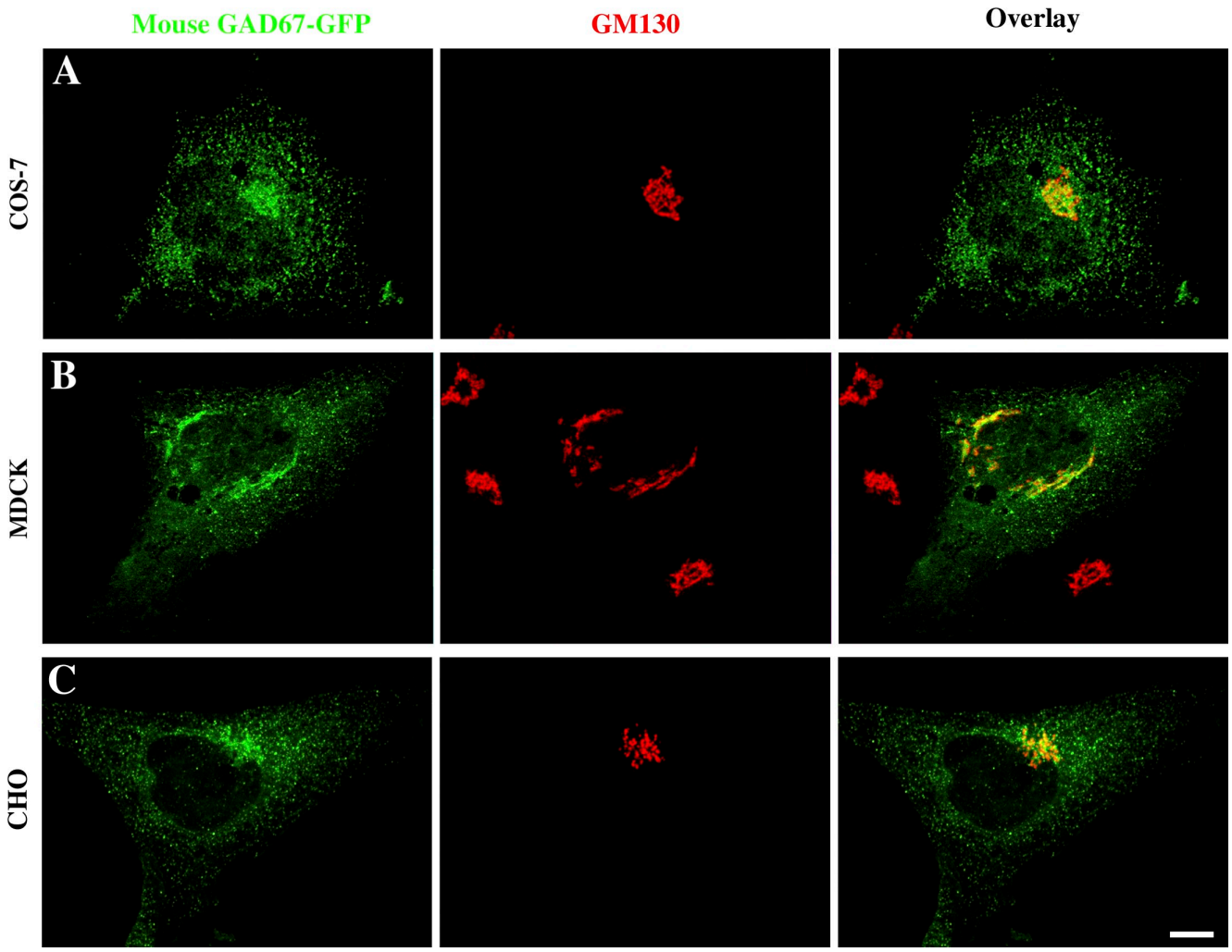

Figure S3. **The GAD65-independent mechanisms of GAD67 membrane anchoring are functional in COS-7, MDCK, and CHO cells.** Projected confocal images of COS-7 (A), MDCK (B), and CHO (C) cells singly transfected with wt mouse GAD67-GFP. Cells were fixed 24 h after transfection and immunostained for GFP (green) and GM130 (red). Mouse GAD67-GFP is targeted to Golgi membranes and cytosolic vesicles in COS-7, MDCK, and CHO cells. Bar, 20 μm.

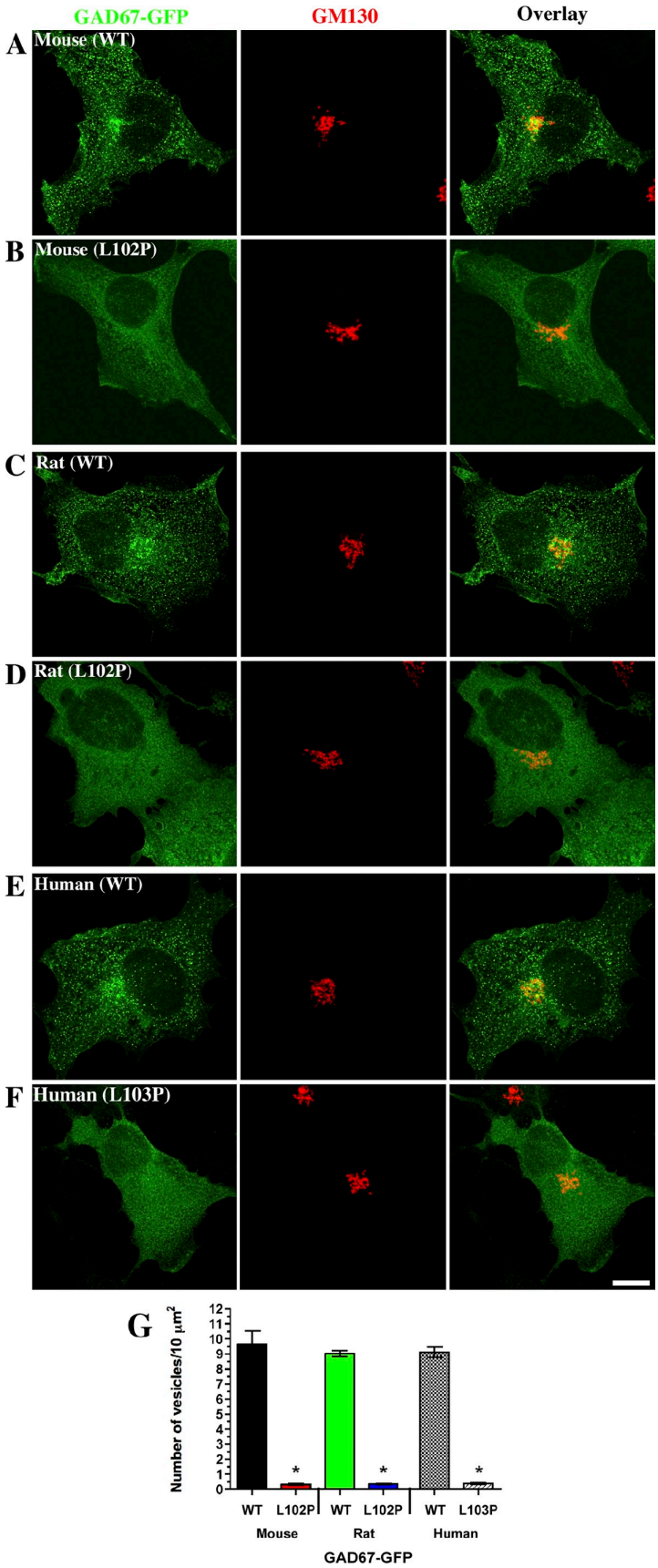

Figure S4. **In COS-7 cells, the leucine-to-proline mutation abolishes targeting of GAD67 to Golgi membranes and cytosolic vesicles in the absence of GAD65.** Projected confocal images of COS-7 cells singly transfected with wt mouse GAD67-GFP (A), mouse GAD67(L102P)-GFP (B), wt rat GAD67-GFP (C), rat GAD67(L102P, V473L)-GFP (D), wt human GAD67-GFP (E), or human GAD67(L103P)GFP (F). Cells were fixed 24 h after transfection and immunostained for GFP (green) and GM130 (red). The L102/103P mutation efficiently inhibits the targeting of mouse, rat, and human GAD67-GFP to Golgi membranes and cytosolic vesicles. Bar, 10 µm. (G) Quantification of the number of GAD67-GFP–containing cytosolic vesicles per 10 µm^2. Results are presented as mean ± SE (error bars) for five cells for each protein. *, $P < 0.0001$.

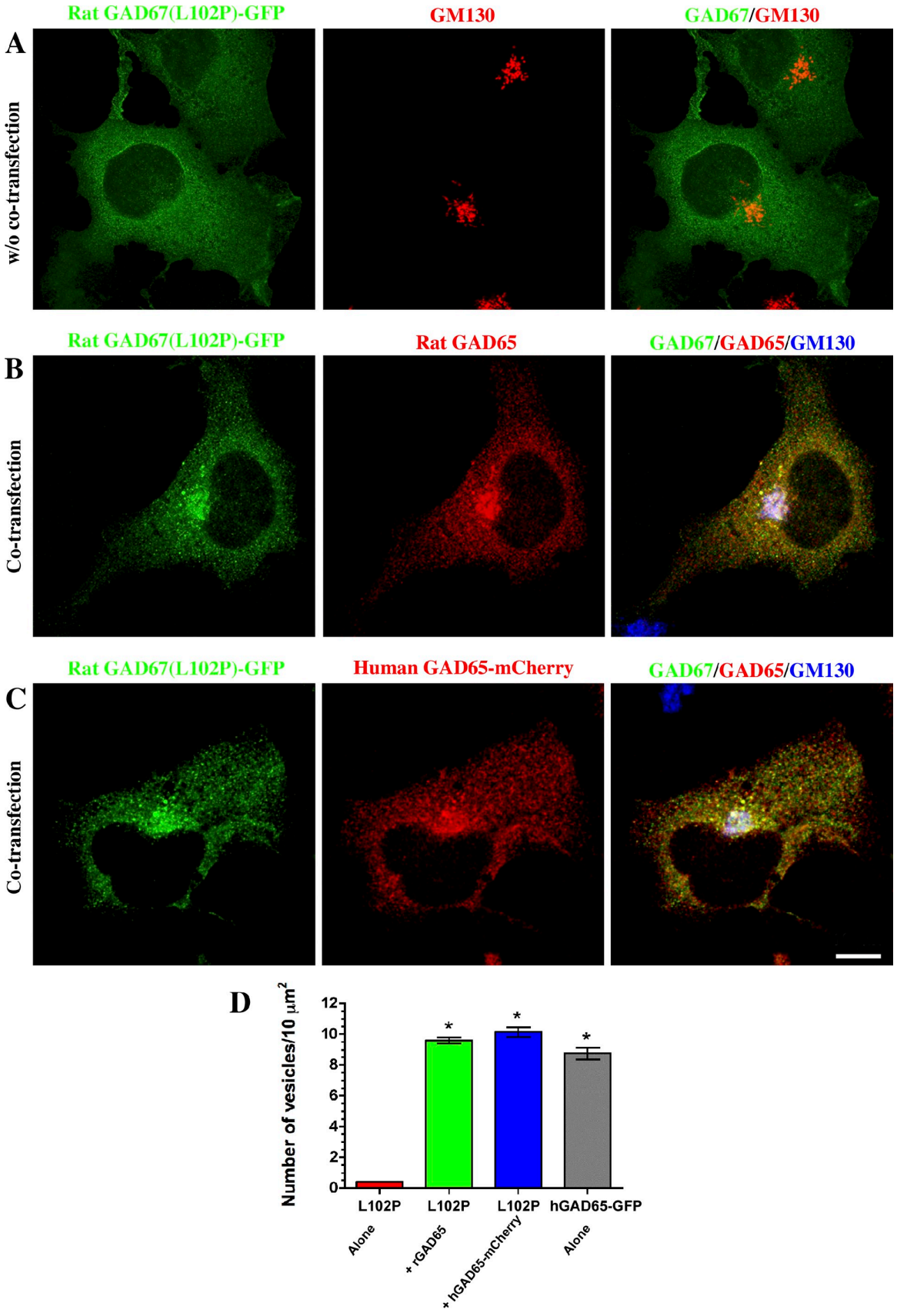

Figure S5. **In COS-7 cells, the GAD65-dependent membrane anchoring of GAD67 is not affected by the L102P mutation.** Confocal images of COS-7 cells singly transfected with a plasmid encoding rat GAD67(L102P, V473L)-GFP and immunostained 24 h after transfection for GFP (green) and GM130 (red; A), or doubly transfected together with either rat GAD65 (B) or human GAD65-mCherry (C) and immunostained 24 h after transfection for GFP (green), GM130 (blue), and either GAD65 with human monoclonal antibodies MICA 2, 3, and 6 (B, red) or mCherry (C, red). Co-expression with either rat GAD65 or human GAD65-mCherry results in targeting of rat GAD67-GFP(L102P)-GFP to Golgi membranes (white in B and C) and cytosolic vesicles. Bar, 10 μm. (D) Quantification of the number of rat GAD67(L102P, V473L)-GFP–containing cytosolic vesicles per 10 μm^2 in COS-7 cells shows a 23.5- and 24.8-fold increase in vesicular targeting of the mutant protein when coexpressed with rat GAD65 and human GAD65-mCherry, respectively. The level of targeting of rat GAD67(L102P, V473L)-GFP to cytosolic vesicles when coexpressed with either rat GAD65 or human GAD65-mCherry is similar to the level of targeting of wt human GAD65-GFP expressed alone. Results are presented as mean ± SE (error bars) for 5–15 cells for each protein. *, $P < 0.0001$.